Steel and Composite Structures, *Vol. 23, No. 5 (2017) 557-570*
DOI: https://doi.org/10.12989/scs.2017.23.5.557

Ambient vibration testing and seismic performance of precast I beam bridges on a high-speed railway line

Burak Toydemir [1a], Ali Koçak [2b], Barış Sevim [*2] and Basak Zengin [2c]

[1] *İstanbul Gelişim University, Gelişim Vocational School, İstanbul, Turkey*
[2] *Yıldız Technical University, Department of Civil Engineering, 34220, İstanbul, Turkey*

(*Received April 25, 2016, Revised January 23, 2017, Accepted*)

Abstract. In this study, the seismic performance levels of four bridges are determined using finite element modeling based on ambient vibration testing. The study includes finite element modeling, analytical modal analyses, ambient vibration testing and earthquake analyses of the bridges. For the purpose, four prestressed precast I beam bridges that were constructed for the Ankara-Sivas high speed railway line are selected for analytical and experimental studies. In the study, firstly a literature review related to the dynamic behavior of bridges especially precast beam bridges is given and then the formulation part related to ambient vibration testing and structural performance according to Turkish Seismic Code (2007) is presented. Next, 3D finite element models of the bridge are described and modeled using LARSA 4D software, and analytical dynamic characteristics are obtained. Then ambient vibration testing conducted on the bridges under natural excitations and experimental natural frequencies are estimated. Lastly, time history analyses of the bridges under the 1999 Kocaeli, 1992 Erzincan, and 1999 Düzce Earthquakes are performed and seismic performance levels according to TSC2007 are determined. The results show that the damage on the bridges is all under the minimum damage limit which is in the minimum damage region under all three earthquakes.

Keywords: ambient vibration testing; dynamic characteristic; finite element modeling; precast I beam bridge; seismic performance level

1. Introduction

Bridges are cultural structures tying the past to the present. They also give information about the time and places they were built. In the past, they were built of wood, stone, and steel materials to pass over short spans on a river or other water ways and the aim of the construction was generally to carry people or other horse-drawn vehicles to carry goods. In the present, bridges can be built to pass spans extending kilometers. They also carry millions of cars and people. So it is more important in the present to design such structures to prevent economic losses, injuries and death.

Bridges can be classified according to material type such as wood, stone, concrete, prestressed reinforced concrete, steel and composite. Also, they can be classified according to structural systems such as beam bridges, arch bridges, cable-stayed bridges, suspension bridges etc. In Turkey, most of the bridges have prestressed precast structural systems. In this type of bridge, simple supported precast beams are replaced by piers, and a continuous system is constituted. Prestressed precast beams have quality casting and faster construction time. However, their high weight and complicated transport and manipulation are their main disadvantages (Moravcik 2013). This kind of bridge can be designed and constructed with developing computer systems and technology. However, deficiencies and inabilities in modeling and building cause damage to the bridges during operation or management, especially under dynamic loading such as earthquakes and winds. So the structural systems of existing bridges have to be controlled at all times.

In structural engineering, modeling and analysis are essential to interpret the behavior of a structure. It is generally expected that finite element (FE) models based on technical design data and engineering judgments can yield reliable simulation for dynamic responses of engineering structures. However, because of modeling uncertainties such as stiffness of supports and non-structural elements such as material properties as well as inevitable differences between the properties of the designed and as-built structures, these finite element models often cannot predict natural frequencies and mode shapes with the required level of accuracy. This raises the need for verification of the finite element models of engineering structures after their construction. One of the important inspections is modal testing to estimate their dynamic characteristics experimentally. The modal testing is necessary to validate the finite element modeling to obtain the actual structural response (Altunışık *et al.* 2011a, b, Heo *et al.* 2014).

Ambient vibration testing is one of the modal testing

∗Corresponding author, Associate Professor,
E-mail: basevim@yildiz.edu.tr
[a] Ph.D. Student, E-mail: btoydemir@gelisim.edu.tr
[b] Associate Professor, E-mail: akocak@yildiz.edu.tr
[c] Ph.D. Student, E-mail: zenginbasak@gmail.com

http://www.techno-press.org/?journal=scs&subpage=6 ISSN: 1229-9367 (Print), 1598-6233 (Online)

methods in which the structure is excited by an unknown input force such as traffic, wind, and seismic loads, and the responses of the structure are measured. The method is usually used around the world to determine the dynamic parameters of bridges such as their natural frequencies, mode shapes and damping ratios. More information related to ambient vibration testing of bridges can be found from the studies published between 2004 and 2015 (Gentile and Bernardini 2008, Bayraktar *et al*. 2009, Kulprapha and Warnitchai 2012, Sousa *et al*. 2013, Schallhorn and Rahmatalla 2015). However, studies related to ambient vibration testing of precast bridges are very limited in the literature. One of the studies, Dwairi *et al*. (2010), presented comprehensive monitoring of the behavior of four prestressed high performance concrete (HPC) bridge girders with higher compressive strength during construction and while in-service. In the study, details of the testing of the concrete properties and field instrumentation of the bridge girders as well as a discussion of service level monitoring and controlled load testing are provided.

Determination of the dynamic response of precast beam bridges or other engineering structures is so important for modeling and dynamic analyses in order to obtain actual response (Ghosh and Singh 2011, Lee *et al*. 2011, El-Gawady and Dawood 2012, Xiao *et al*. 2012, Marti *et al*. 2013, Kim *et al*. 2015, Kong *et al*. 2015).

In Ryu and Chang (2005), several experiments and analytical studies were performed in order to apply precast decks to continuous composite bridges. For the purpose, experimental and analytical studies of two-span continuous composite bridges with open box girder sections were conducted. Cracking, yielding and ultimate loads were evaluated and compared with the test results for the design of continuous composite bridges with precast decks. Roh and Reinhorn (2010) suggested an alternative method to increase the energy dissipation capacity of post-tensioned (PT) segmental bridge piers. In this method, the use of superelastic shape memory alloy (SMA) bars is used in order to improve the hysteretic performance including the energy dissipation capacity of the bridge columns. Dawood and El-Gawady (2013) presented a seismic design procedure for self-centering precast post-tensioned bridge piers. The piers presented in the study consisted of concrete-filled fiber reinforced polymer tubes. Different performance criteria were proposed for the system according to the intensity and the frequency of occurrence of a seismic event. The developed empirical equations were arranged to achieve a given performance level for a specific seismic zone. Sarrazin *et al*. (2013) studied the effect of seismic isolation on the dynamic response of precast prestressed bridges in Chile which were exposed to a huge earthquake with 8.8 magnitude. Analyses were performed using the acceleration records obtained at the bridges. From the study, the beneficial effect of the isolation system, especially in the longitudinal direction, was highlighted. Asr *et al*. (2014), presented an approach to create a structured polynomial model for predicting the undrained lateral load bearing capacity of piles. The proposed evolutionary polynomial regression (EPR) technique is an evolutionary data mining methodology that generates a transparent and structured representation of the behavior of a system directly from raw data. In the study, the merits and advantages of the proposed methodology were discussed. Casas and Chambi (2014) studied the methodology for a reliability-based calibration of the partial safety factors to be used for confined concrete in the design of strengthening against axial-bending forces using CFRP. In the study, a simple set of partial safety factors is proposed and compared with those proposed in existing guidelines. Mara *et al*. (2014) aimed to examine the sustainability of these FRP solutions in comparison with traditional bridge concepts. An existing composite (steel–concrete) bridge with a concrete deck that had deteriorated was selected for this purpose. It was concluded from the study that FRP decks contribute to potential cost savings over the life cycle of bridges and a reduced environmental impact. Roh *et al*. (2014) presented an alternative modeling technique for post-tensioned (PT) rocking bridge piers connected with energy dissipation (ED) bars, and investigated the effect of yielding strength level and post-yielding stiffness ratio of ED bars on the seismic response of PT rocking bridge piers. They learned from the study that the use of ED bars with higher yielding moment strength decreases the peak displacement while it increases the peak acceleration response. Mayoral and Romo (2015) studied the dynamic response of vehicular overpasses with massive foundations built in highly populated earthquake prone regions to assess the massive foundation potential of being a technically sound means to reduce the structural response during major earthquakes. It was emphasized from the study that the massive foundations seem to be a convenient alternative to reduce the overall structural seismic response. Yan *et al*. (2015) presented a brief historical review of high speed railway development. For the purpose, design concepts and structural dimensions of two typical spans are discussed, including the superstructure and substructure as well as the auxiliary facilities on the bridge deck. Valipour *et al*. (2015) presented the results of the testing of precast concrete slabs in a deconstructable composite steel–concrete system for the construction of bridge decks. In the study, Benign arching action is utilized to carry the point (wheel) loads to the supports and to develop the required slab capacity; and the failure mode and load–deflection response of precast concrete slabs were investigated. Highlighted in the study was that the arching effect in the slabs is very beneficial and cannot be ignored in rational structural design processes.

Camara and Astiz (2012) studied the seismic response prediction of cable-stayed bridges under multi-directional excitation using pushover analysis. For the purpose, finite element models of different cable-stayed bridges constituted with different span lengths, tower shapes and class of foundation soil as well as seismic response of the models using modal pushover analysis and a new coupled pushover analysis, are determined. In Karmakar *et al*. (2012) a three-dimensional finite element model of the Vincent Thomas Bridge is developed. In order to show the appropriateness of the model, the eigen properties of the bridge model are evaluated and compared with the results of system identification from ambient vibration and the 2008 Chino Hills' earthquake response data. A new simulation technique was developed to generate spectrum-compatible spatial variable ground motions. The response of the Vincent Thomas Bridge, under spatially varying ground motion, is evaluated by nonlinear time history analysis. Park and Towashiraporn (2014) represented a new method for rapid estimation of the seismic damage to track-on-steel-plate-girder (TOSPG) bridges so that a seismic risk analysis of a TOSPG bridge with an arbitrary physical configuration can be effectively performed without significant loss of time or effort. Highlighted is that the approach developed in this study can be effectively applied for making macro-level decisions on seismic retrofit through flexible estimation of the seismic damage and fragility of arbitrarily selected structures in a given class because the simulation is performed not with a number of time–history nonlinear dynamic analyses but with simple numerical equations. Mayoral and Romo (2015) investigated the earthquake response of bridges with massive foundations built in highly populated earthquake prone regions. In the study, a 3D finite element model of a bridge in Mexico City was constituted using SASSI2000 software. The main aim of the study was to show the seismic performance evaluation of massive foundations used as an alternative to positively modify the dynamic response. In the study, it is concluded that the massive foundations seem to be a convenient alternative to reduce the overall structural seismic response. Wilson *et al*. (2015) assessed the effect of vertical ground motion on a horizontally skewed and curved highway bridge for a moderate-to-high seismic region. A numerical model of a skewed and curved, three-span bridge located in Tacoma, Washington is subjected to a suite of horizontal and vertical ground motion using non-linear time-history analysis. The results showed that excluding the vertical ground motion component from the analyses may impose a larger margin of risk than previously perceived, which is particularly the case for moderate-to-high seismic regions where shorter period bridges may resonate with predominant frequencies of vertical ground motion.

On the other hand, there are several standards in the world for the design of bridges, and dynamic analysis methods should be included in these standards to evaluate and ensure the safety of structures (TSC 2007). All of these analysis methods are based on using the dynamic characteristics of the structures. As a result, accurate determination of the dynamic characteristics of a structure is of great importance. Due to priorities based on cost or strategic importance of the bridges, determining the actual response is vital. So modeling and analyzing the bridges during the operational stage for seismic activity, has greater importance. After dynamic analyses of the structure, performance level should be estimated according to the standards.

According to the literature review, researchers still recommend the investigation of seismic behavior of all types of bridge, analytically and epically experimentally. However, studies related to prestressed precast bridges based on seismic performance levels are few. So, in this study, the seismic performance levels of four bridges according to Turkish Seismic Code (2007) are determined using finite element modeling based on ambient vibration testing. The study includes finite element modeling, analytical modal analyses, ambient vibration testing, and earthquake analyses of these bridges. The bridges selected for the study have precast I beam structural systems and are on the high speed Ankara-Sivas railway line which is in the middle region of Turkey. First, a general literature review related to the modal behavior of the bridge is given above. Then a formulation part related to ambient vibration testing and structural performance according to Turkish Seismic Code (2007) is presented. After that, the four bridges are introduced, the finite element modeling and ambient vibration testing of which are presented. Lastly, earthquake analyses are performed and structural performance is determined according to TSC2007.

2. Formulation

In this study, dynamic characteristics of the four bridges obtained from ambient vibration testing are estimated using Enhanced Frequency Decomposition Domain Technique. Before estimating the modal parameters Detrending and Butterworth Functions are used to filter un-structural vibrations. The earthquake responses of the bridges are obtained from time history analyses. In the time history analyses, the equations of motion are solved using the Newmark Algorithm (Bathe 1996, Chopra 2006). The structural performance of the bridges according to time history analysis results is assessed using performance levels given in Turkish Seismic Code 2007. The bases of the techniques are summarized below:

2.1 Enhanced frequency decomposition domain technique

Ambient Vibration Testing (AVT) has succeeded in attracting a lot of attention since the 1980s. AVT is a form of analysis that determines the dynamic characteristics of the structure during operational stage. In AVT, the loads that cause the dynamic responses are created by pedestrian movements, vehicle loads, wind loads and micro-tremors. In AVT, the size and the forces that cause the vibrations are unknown. Thus, it is also called Output Only Modal Analysis because the response of the structure during AVT gives an accurate starting point for dynamic analysis of the structure.

There are several techniques to estimate the modal parameters of the structure in AVT. One of these techniques is Enhanced Frequency Domain Decomposition (EFDD). In EFDD, the single degree of freedom (SDOF) Power Spectral Density (PSD) function, identified around a peak of resonance, is taken back to the time domain using the Inverse Discrete Fourier Transform (IDFT). The natural frequency is obtained by determining the number of zero-crossings as a function of time, and the damping by the logarithmic decrement of the corresponding SDOF normalized auto correlation function. In the EFDD technique, the relationship between the unknown input $x(t)$ and the measured responses $y(t)$ can be expressed as (see Brincker *et al*. 2000, 2003, Bendat and Piersol 2004, Jacobsen *et al*. 2006)

$$\left[G_{\mathbf{yy}}(j\omega)\right]=\left[H(j\omega)\right]^{*}\left[G_{\mathbf{xx}}(j\omega)\right]\left[H(j\omega)\right]^{T} \tag{1}$$

where $G_{xx}(jw)$ is the rxr Power Spectral Density (PSD) matrix of the input; r is the number of inputs; $G_{yy}(jw)$ is the mxm PSD matrix of the responses; m is the number of responses, $H(jw)$ is the mxr Frequency Response Function (FRF) matrix; and * and superscript T denote complex conjugate and transpose, respectively (Brincker *et al*. 2000).

The FRF can be written in partial fraction, i.e., pole/residue form

$$H(jw)=\sum_{k=1}^{n}\frac{R_k}{jw-\lambda_k}+\frac{R_k^{*}}{jw-\lambda_k^{*}} \tag{2}$$

where n is the number of modes, λ_k is the pole and R_k is the residue. Then Eq. (1) becomes (Brincker *et al*. 2000)

$$G_{yy}(jw)=\sum_{k=1}^{n}\sum_{s=1}^{n}\left[\frac{R_k}{jw-\lambda_k}+\frac{R_k^{*}}{jw-\lambda_k^{*}}\right][G_{xx}(jw)]\left[\frac{R_s}{jw-\lambda_s}+\frac{R_s^{*}}{jw-\lambda_s^{*}}\right]^{H} \tag{3}$$

where s are the singular values and superscript H denotes complex conjugate and transpose. Multiplying the two partial fraction factors and making use of the Heaviside partial fraction theorem, after some mathematical manipulations, the output PSD can be reduced to a pole/residue form as follows (Brincker *et al*. 2000).

$$G_{yy}(jw)=\sum_{k=1}^{n}\frac{A_k}{jw-\lambda_k}+\frac{A_k^{*}}{jw-\lambda_k^{*}}+\frac{B_k}{-jw-\lambda_k}+\frac{B_k^{*}}{-jw-\lambda_k^{*}} \tag{4}$$

where A_k is the kth residue matrix of the output PSD. In the EFDD identification, the first step is to estimate the power spectral density matrix. The estimate of the output PSD $\hat{G}_{yy}(jw)$ known at discrete frequencies $w = w_i$ is then decomposed by taking the SVD of the matrix (Brincker *et al*. 2000, Herlufsen *et al*. 2006).

$$G_{yy}(jw_i)=U_iS_iU_i^{H} \tag{5}$$

where the matrix $U_i = [u_{i1}, u_{i2},..., u_{im}]$ is a unitary matrix holding the singular vectors u_{ij}, and S_i is a diagonal matrix holding the scalar singular values s_{ij}. Thus, in this case, the first singular vector u_{ij} is an estimate of the mode shape. PSD function is identified around the peak by comparing the mode shape estimate u_{ij} with the singular vectors for the frequency lines around the peak. As long as a singular vector is found that has a high Modal Assurance Criterion (MAC) value with u_{ij}, then the corresponding singular value belongs to the SDOF density function (Brincker *et al*. 2000).

From the pieces of the SDOF density function obtained around the peak of the PSD, the natural frequency and damping can be obtained. The pieces of the SDOF PSD are taken back to time domain by inverse FFT, and the frequency and the damping are simply estimated from the crossing times and the logarithmic decrement of the corresponding SDOF auto correlation function (Brincker *et al*. 2000).

In the case where two modes are dominating, the first singular vector will always be a good estimate of the mode shape of the strongest mode. However, in case where the two modes are orthogonal, the first singular vectors are unbiased estimates of the corresponding mode shape vectors (Brincker *et al*. 2000).

2.2 Detrending and butterworth functions

A spectral analysis is dependent upon the statistical characteristics of the data being analyzed. If the data are aperiodic and non-stationary, major problems are encountered. The detrending and filtering methods are used to remove low frequency and aperiodic non-stationary components from the time series. The filters transform one time series into another. The frequency domain modification of the time series by the filter is called a transfer function. The transfer function provides information regarding the filter's ability to block, attenuate, and amplify specific frequencies within the spectrum.

The detrending methods remove non-stationary influences and perform other high-pass functions. The detrending filter needs to have a number of characteristics to successfully perform. First, the filter must be able to remove non- stationary trend from the time series. Second, the filter should have a sharp cut-off so the non-stationary and low frequency variations are completely removed without distorting the frequency and amplitude components of the periodicity being studied. Third, since periodic physiological activity can seldom be described by a single sine wave, the filter should have the ability to remove the influences of slow processes which, although periodic, may have component variances in the frequency band of the periodicity of interest. Fourth, the transfer function of the filter should be predictable for all applications.

One practical way of assessing the transfer function of a filter is to observe the impact of the filter on a white noise time series. Since white noise is defined as a time series with the expected value of the spectral densities being the same for all frequencies, the spectrum of white noise should theoretically be flat. With knowledge of the spectral characteristics of a white noise time series, the transfer function of the filter on the spectrum can be evaluated by comparing the filtered spectral densities to the white noise spectrum. If the original white noise spectrum is divided into the filtered spectrum, it would be better able to estimate the transfer function. If the numbers at specific frequencies approximate 1.0, the filter provides an accurate description of periodicity. If the numbers are less than 1.0, the filter attenuates the spectral densities. If the numbers approach 0.0, the filter rejects specific frequencies. If the numbers are greater than 1.0, the filter amplifies specific frequencies.

In this study a linear detrending method is used to remove white noise. This is done by fitting a linear regression to the data. This method removes linear influences and transforms the data set into a series with mean of approximately zero. Linear detrending has little impact on the spectrum of white noise. However, if the white noise series had been superimposed on a large linear trend, the spectral decomposition of this series would distribute most of the variance at 0.0 Hz in the spectrum. A spectrum with a relatively large proportion of the variance at 0.0 Hz is characteristic of a time series with non-stationary components. If the non-stationarity is caused by a linear trend, linear detrending will remove the non-stationary influence and provide an interpretable spectrum. Unfortunately, the non-stationary influences in a physiological times series seldom fit with a linear regression. Routine application of linear and other low order polynomial fits (e.g., quadratic, cubic, etc) to the entire data set, seldom achieves the anticipated goal of removing non-stationary influences.

The Butterworth filter is a type of signal processing filter designed to have as flat a frequency response as possible in the passband. It is also referred to as a maximally flat magnitude filter. It was first described in 1930 by the British engineer and physicist Butterworth (1930).

Butterworth showed that a low pass filter could be designed, whose cutoff frequency was normalized to 1 radian per second and whose frequency response (gain) was

$$G(w)=\sqrt{\frac{1}{1+w^{2n}}} \tag{6}$$

where ω is the angular frequency in radians per second and n is the number of poles in the filter, equal to the number of reactive elements in a passive filter.

2.3 Bases of linear seismic performance according to Turkish Seismic Code 2007

The most important advantage of a time history analysis is that the load can be varied based on time and as a result real seismic records can be used as loads which can be understood from the equations. In order to use the seismic record, the records from The Ministry of Environment and Urban Planning Seismic Research Institute 15 or the records from Pacific Earthquake Research (PEER) Center 16 can be used. The records can be used as is or after an adjustment based on the location of the structure according to the response spectrum calculated by the seismic code. In the case of not using any real seismic record, a seismic record can be created by using random vibrations which are stable except at the beginning and the end and can be used in the dynamic analysis (Catalan *et al*. 2010, Kayhan *et al*. 2011, Zacharenaki *et al*. 2014).

During this study, it is assumed that the structural characteristics will remain unchanged and linear time history analysis will be performed on the structures. Real seismic records will be used for time history analysis after adjusting the records according to the seismic code. The linear seismic performance of the structure will be evaluated based on the loading of the adjusted seismic records.

After the time history analyses are conducted, the element forces, the K_N, and K_V performance factors, and *r* capacity ratio are calculated and evaluated based on the Turkish Seismic Code (2007).

Table 1 Seismic performance levels according to TSC2007

Ductile sections			Performance levels (*r*)		
K_N	Confinement	K_V	ML	SL	CL
≤ 0.1	Yes	≤ 0.65	3	6	8
≤ 0.1	Yes	≥ 1.30	2.5	5	6
≥ 0.4 and ≤ 0.7	Yes	≤ 0.65	2	4	6
≥ 0.4 and ≤ 0.7	Yes	≥ 1.30	1.5	2.5	3.5
≤ 0.1	No	≤ 0.65	2	3.5	5
≤ 0.1	No	≥ 1.30	1.5	2,5	3.5
≥ 0.4 and ≤ 0.7	No	≤ 0.65	1.5	2	3
≥ 0.4 and ≤ 0.7	No	≥ 1.30	1	1.5	2
≥ 0.7	-	-	1	1	1

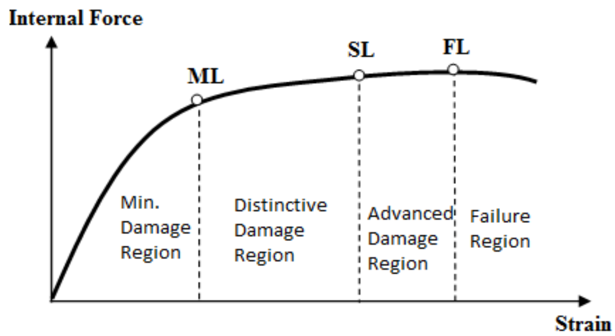

Fig. 1 Damage limits and regions based on Turkish Seismic Code 2007

$$K_N=\frac{N_K}{A_c.f_{cm}} \quad \text{and} \quad K_V=\frac{V_e}{b_{w.d}.f_{ctm}} \tag{7}$$

where A_c, is the cross section area; b_w, width of the section; *d*, useful height; f_{cm}, concrete compression strength; f_{ctm}, concrete tensile strength, N_K, axial load capacity; *Ve*, design shear force (shear force capacity); and *r*, the ratio between moments caused by seismic loads and the difference between the moment capacity of the section and moments caused by vertical loads. The capacity ratio of the section is as follows

$$M_A=M_K-M_D \quad \text{and} \quad r=\frac{M_E}{M_{A.}} \tag{8}$$

where; M_K, is the bending moment capacity of the section; M_A, residual bending moment capacity; M_D, bending moment caused by vertical loads; and M_E, bending moment caused by seismic loads. Calculated capacity ratios are used to determine the seismic performance levels of the structures based on Table 1 and the corresponding damage levels are shown in Fig. 1. In Table 1 and in Fig. 1, ML, SL, and FL show the minimum damage limit, the safety damage limit, and the failure damage limit, respectively.

3. Fem, Avt and seismic performance of precast I beam bridges

Turkey has been making great investments in High Speed Trains in order to connect the major cities with each

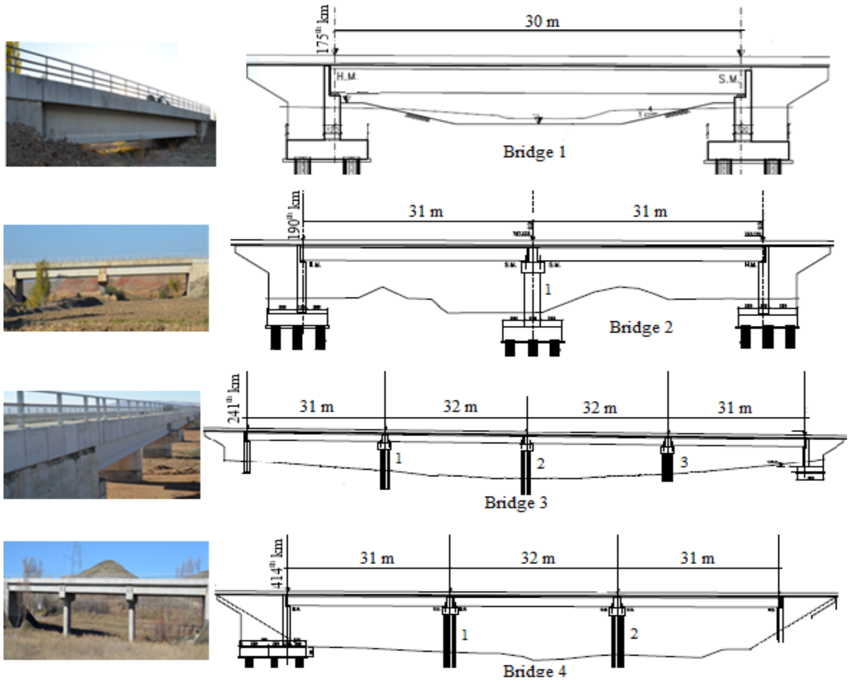

Fig. 2 Geometrical properties of the bridges

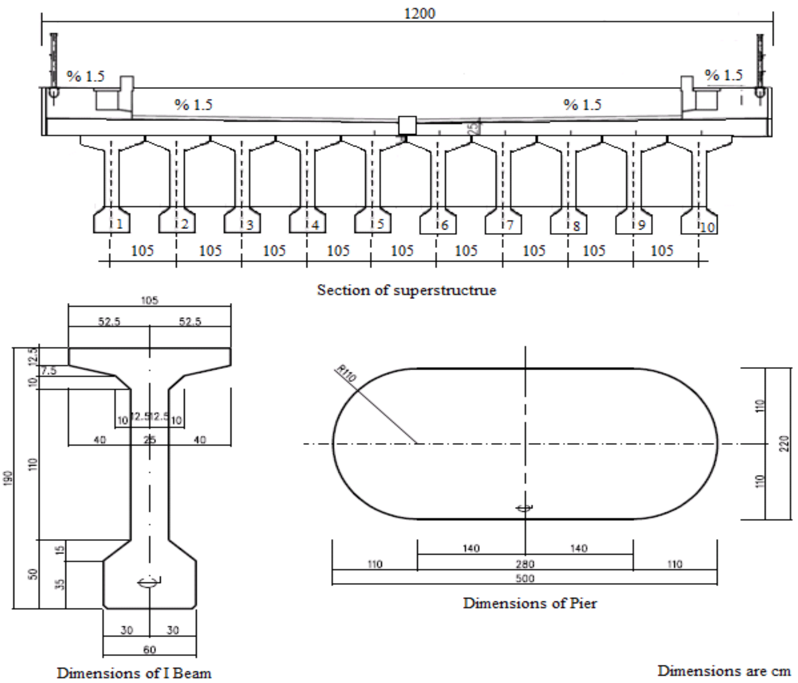

Fig. 3 Section of superstructure, dimensions of I beam, and dimension of piers of the bridges

other. One of the most important sections of these high speed railways is the connection between Ankara (the capital) and Sivas which is in the Middle Eastern part of Turkey. There are several railway bridges on this line and in this study four of these bridges with different sizes and spans have been studied for dynamic characteristics and seismic performance. The geometrical spans of the bridges are given in Fig. 2. As seen in Fig. 2; Bridge 1 is in the 175^{th} km of railway line and has one span; Bridge 2 is in the 190^{th} km of railway line and has two spans; Bridge 3 is in the 241^{st} km of railway line and has four spans; and Bridge 4 is in the 414^{th} km of railway line and has three spans. The lengths of the bridges change from 30 m to 124 m.

The superstructure of the bridges is the same for each. The bridge superstructure has 10 AASHTO Type 6 prestressed precast I beam girders connecting the abutments. 55 cm of C25 concrete are placed on the girders to create the deck and two sets of UIC60 rails are fixed on top of the concrete to complete the superstructure of the bridges (See Fig. 3). The precast I beam girders are

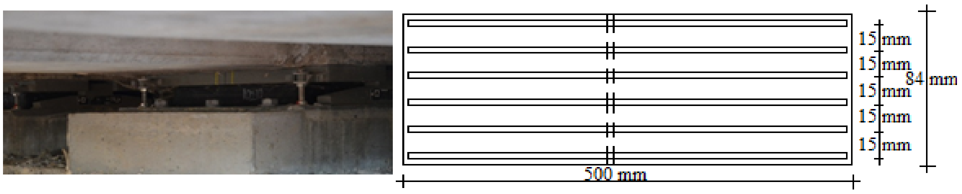

Fig. 4 Elastomeric bearing on abutments and its section properties

Table 2 Material properties using finite element analysis of the bridges

Parts	Elasticity modulus (N/mm^2)	Poisson ratio	Density (kg/m^3)
Deck	3.0E10	0.17	2360
Precast I Beams	3.4E10	0.17	2360
Abutments	3.0E10	0.17	2360
Piers	3.0E10	0.17	2360

supported by elastomeric bearings on the abutments and the section properties of the bearing are given in Fig. 4. The elastomeric bearing has rigidities with 6211000 kN/m in the lateral direction and 26800000 kN/m in the vertical direction. The sections of the piers are the same for each bridge (See Fig. 3), but the heights of the piers differ. Bridge 2 has a pier with 15 m height; Bridge 3 has three piers with 17, 17, and 14 m heights; and Bridge 4 has two piers with 19 m heights.

3.1 Finite element modeling and analytical dynamic characteristics

The three dimensional (3D) finite element models (FEM) of the bridges were constituted using commercial software called LARSA 4D (2013) Bridge Series. LARSA 4D (2013) is a structural analysis software specifically designed to analyze bridges and has the ability to model prestressed precast girder bridges including sub and superstructures. It also considers elastomeric bearings on the model and geometrical nonlinearity is taken into account in time history analyses. The material properties used in the analysis are listed in Table 2. The 3D FEMs of the bridges and dynamic characteristics such as natural frequencies and mode shapes obtained from LARSA 4D (2013) are illustrated in Fig. 5. In Fig. 5, the first three natural frequencies and mode shapes for each bridge are represented. As seen in Fig. 5, the first three natural frequencies for all bridges change between 0.12 and 0.62 s and the mode shapes are vertical bending, longitudinal bending and torsional modes. Detailed natural frequencies and periods are listed in Table 3. As seen in Table 3, the first

Table 3 Natural frequencies and periods of the bridges

Modes	Bridge 1 (175th km)		Bridge 2 (190th km)		Bridge 3 (241th km)		Bridge 4 (414th km)	
	Freq. (Hz)	Period (s)	Freq. (Hz)	Period (s)	Freq. (Hz)	Period (s)	Freq. (Hz)	Period (s)
1	3.53	0.28	2.49	0.40	1.62	0.62	2.21	0.45
2	5.34	0.19	3.48	0.29	3.13	0.32	2.40	0.42
3	8.56	0.12	5.64	0.18	3.42	0.29	3.15	0.32
4	18.43	0.05	10.75	0.09	4.60	0.22	3.96	0.25
5	22.89	0.04	14.25	0.07	5.34	0.19	5.05	0.20

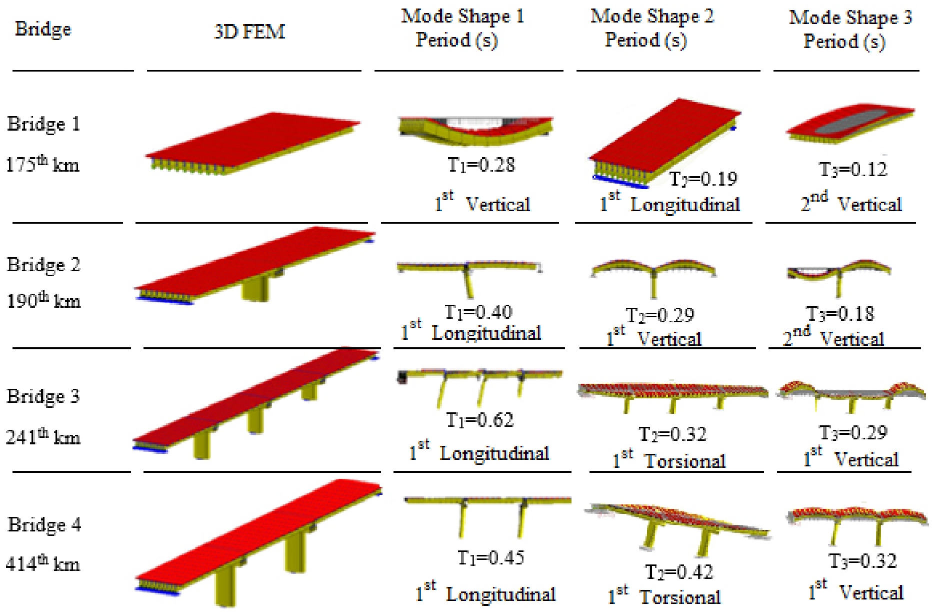

Fig. 5 3D FEM, the natural frequencies and the modes shapes of the bridges

Fig. 6 Uni-axial accelerometer and data acquisition system used during ambient vibration testing of the bridges

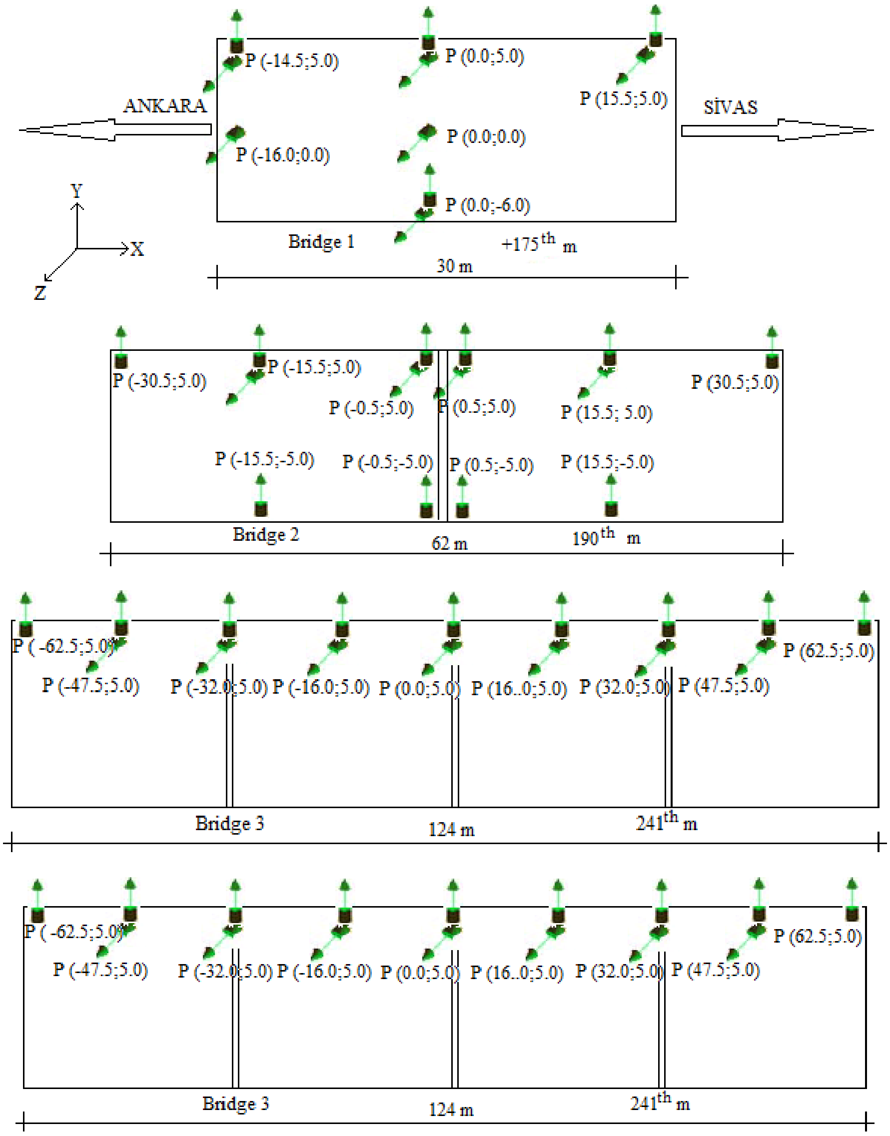

Fig. 7 Location of accelerometers used during ambient vibration testing of the bridges

three modes in all three directions have an important role on the seismic response of the bridges.

3.2 Ambient vibration testing and experimental dynamic characteristics

Ambient vibration tests were conducted on the bridges to determine their natural frequencies. An important point in vibration tests is the selection of measurement equipment (especially accelerometer type) and the measurement setup such as measurement time and frequency span because the measurement equipment and setup vary depending on the tested structure type. For example, accelerometers, frequency span, and measurement time, which are used for the vibration test of a small structure, must not be used for the vibration test of a large structure because the results cannot be accepted. In the ambient vibration tests, TESTBOX 2010 was used as the data acquisition device. The device has 24 Bit ADC resolution with simultaneous sampling capability and 138 dB dynamic range. The device can sample 16 different channels. Sensebox 702X series accelerometers were used to collect data from the bridges. The type of the accelerometers gives force/ electro-dynamic feedback. Maximum acceleration measurement interval is 3 g, Noise Density is 130 ng/√Hz, and the sensitivity of the accelerometers is between 2400 and 6000 mV/g. Temperature working conditions are between -40°C and ~ +65°C. When considering well suited signals, one of the important parameters is the duration of the tests. In the literature, some studies related to testing time have been done. For instance, Bendat and Piersol (1986) explained the minimum 17 minutes for the tests. Caetano (2000) determined the time as 240-1280 times the highest period of the structure. Ramos (2007) in his studies, determined the time as a minimum of 10 minutes and 1000 times the highest period of the structure. The sampling rate defines the upper limit of the frequency band and it is the number of data samples acquired per unit of time.

In this study, the measurements were performed for 30 min, and excitations were provided from natural vibrations with the 200 Hz sampling ratio. In the tests, frequency span was selected as 0–15 Hz according to the finite element modeling results. During each of the tests, uni-axial and bi-axial accelerometers (see Fig. 6) were used in order to collect the signal data to send to the data acquisition system which is shown in Fig. 6. The locations of the accelerometers for ambient vibration testing of each bridge are illustrated in Fig. 7. Signals obtained from the tests were processed by commercial software and ARTEMIS (2014). The dynamic characteristics of the bridges were extracted by EFDD technique.

In estimating the natural frequencies obtained, ambient vibration testing, detrending function and Butterworth

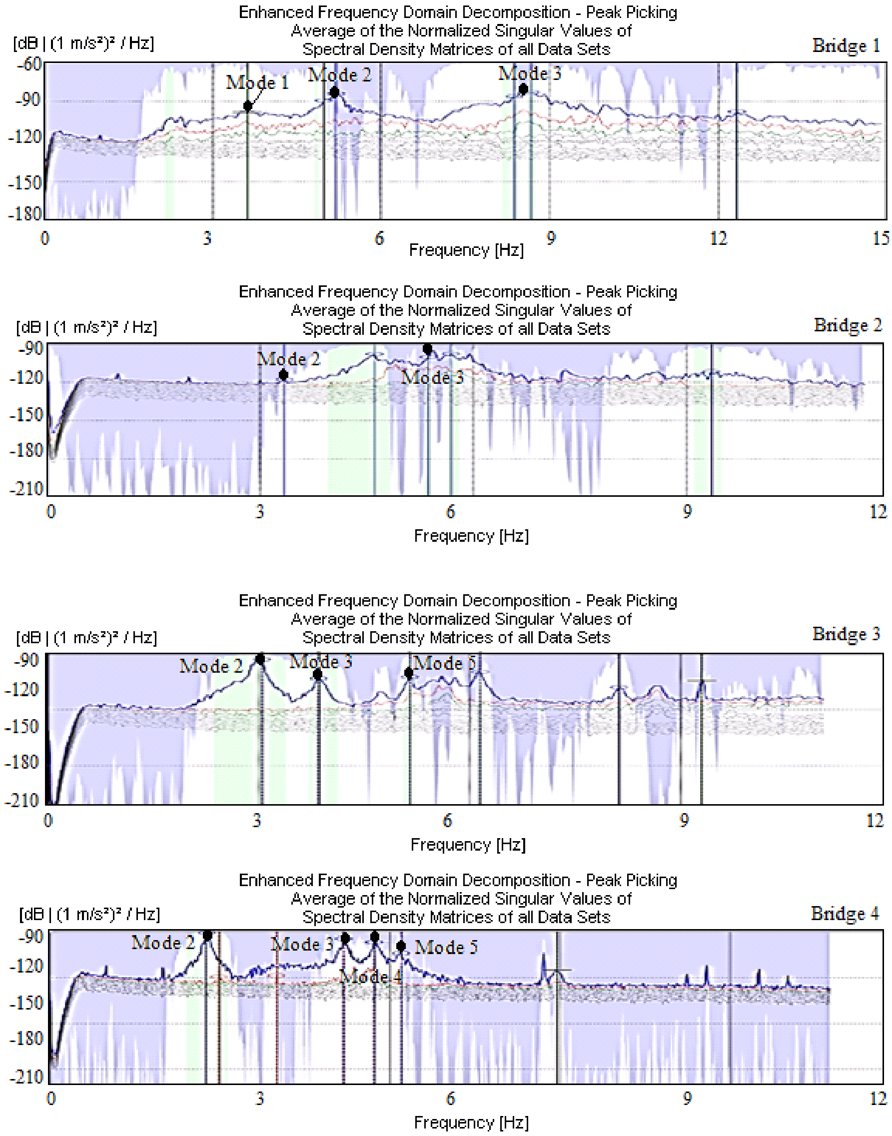

Fig. 8 The singular values and estimation of frequencies of modes for each bridge

Table 4 Experimental natural frequencies and damping ratios of the bridges

Modes	Bridge 1 (175th km)		Bridge 2 (190th km)		Bridge 3 (241st km)		Bridge 4 (414th km)	
	Freq. (Hz)	Damping ratio (%)	Freq. (Hz)	Damping ratio (%)	Freq. (Hz)	Damping ratio (%)	Freq. (Hz)	Damping ratio (%)
1	3.45	2.99	-	-	-	-	-	-
2	5.41	2.39	3.53	2.56	3.10	1.74	2.42	2.55
3	8.58	0.32	5.61	0.98	3.56	2.22	3.12	1.11
4	-	-	-	-	4.68	0.85	4.12	0.93
5	-	-	-	-	5.42	0.70	5.18	0.82

function between 0.5 Hz–15 Hz were used to filter the data. Detrending the data is a necessary function to get more accurate results while converting a signal which is collected in a designated time period, from time domain to frequency domain. Fourier transformation is applied to the signal by dividing signal by finite lengths, and different linear trends in these separated time periods could create deflection of the results. It is sufficient and practical to control the frequencies between 0.5 Hz and 10 Hz which are extracted from the ambient vibration testing with the frequencies collected from 3D modeling of the structure at the same frequency range. In order to filter the frequencies out of 0.5 Hz and 10 Hz, Butterworth Bandpass filter was applied to the signals and the out of range frequencies were cleared from the signal. The filter order is kept to minimum values so as not to lose any signal without compromising the integrity of the signal.

Filtered signals have been analyzed using the Structural Vibration Solutions Artemis Modal Software (ARTEMIS 2014). In the analysis, Enhanced Frequency Domain Decomposition (EFDD) technique was used. The signal and the locations of the collected signals were loaded to the software and the signals filtered. After completing these steps, frequency density functions were calculated by the software and single value decomposition graphs were calculated. The singular values of the spectral density matrices (SVSDM) of the data set and estimation of frequencies of modes for each bridge are illustrated in Fig. 8. The natural frequencies and damping ratios obtained from ambient vibration testing for each bridge are listed in Table 4. As seen in Table 4, the first three natural frequencies changed between 0 and 12 Hz. Also the damping ratios changed between 0 and 3%.

3.3 Seismic performance levels of the bridges according to TSC 2007

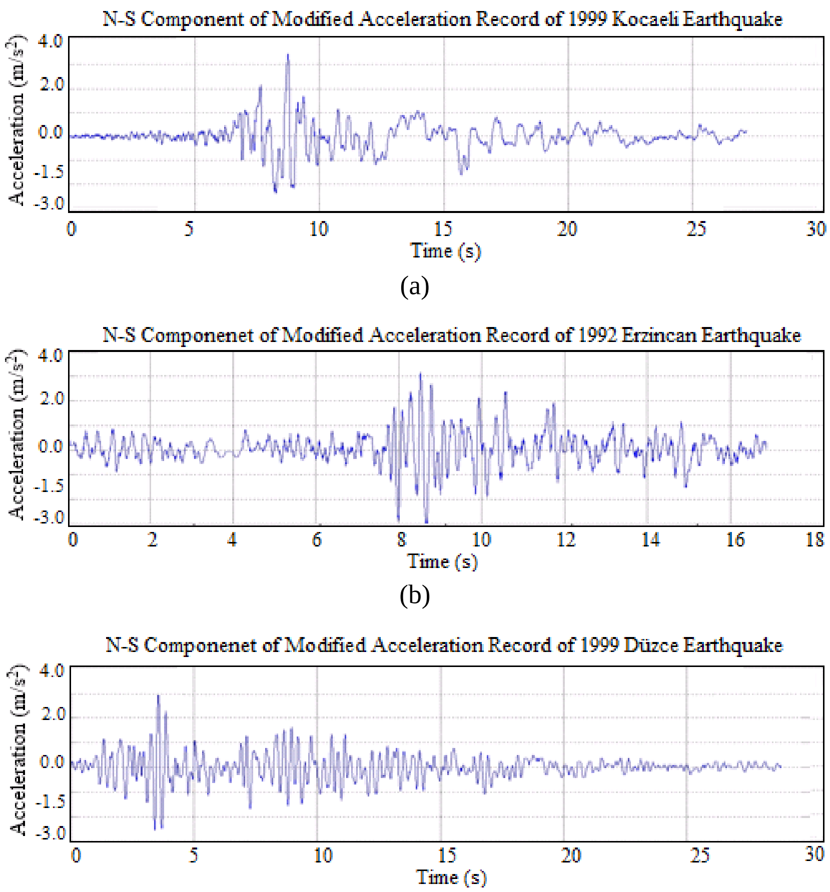

(c)

Fig. 9 (a) Modified time-history of ground motion acceleration of 1999 Kocaeli Earthquake; (b) Modified time-history of ground motion acceleration of 1992 Erzincan Earthquake; (c) Modified time-history of ground motion acceleration of 1999 Düzce Earthquake

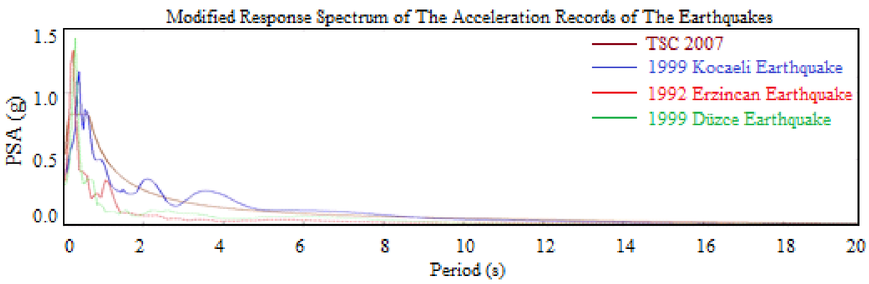

Fig. 10 Modified response spectrums of the acceleration records of the earthquakes

As can be seen from Tables 3 and 5, there is little difference between the analytical and experimental results compared to the natural frequencies. So it is not necessary to update the 3D finite element model of the bridge, and the initial models seem to be accurate. So the finite element models were used in the earthquake analyses of the bridges. Here it is important to recall that due to the locations of the accelerometers during the tests, the modes through X direction are not estimated.

The 1999 Kocaeli Earthquake, 1992 Erzincan Earthquake and 1999 Duzce Earthquake records were used for the time history analysis. All of the earthquakes took place on the North Anatolian Fault in Turkey. The bridges are on the Ankara-Sivas Railway line which is also in the North Anatolian Fault Area. The seismic records were adjusted using the response spectrum according to soil types and seismic regions where the bridges are located. In this study, the seismic load, which has a 2% probability of being exceeded in 50 years, is used as input on the bridges. The real seismic data for the earthquakes are taken from Disaster and Emergency Management Presidency (2015) and the response spectrum of the earthquakes was calculated. The calculated response spectrum and the response spectrum mandated by TSC2007 were compared and α factor was calculated as

$$\alpha = \frac{\sum_{T=T_A}^{T_S} (S_A^{real}(T)\cdot S_A^{TSC}(T))}{\sum_{T=T_A}^{T_S} (S_A^{real}(T))^2} \tag{9}$$

where $S_A^{real}(T)$, the PSA from Real Seismic Data and $S_A^{TSC}(T)$, the PSA from Turkish Seismic Code α factor for earthquakes were calculated and real seismic records were adjusted based on the calculated α factor. The 1999 Kocaeli, 1992 Erzincan and 1999 Düzce Earthquakes' modified acceleration records are illustrated in Figs. 9(a)-(c), respectively. The modified response spectrums of the three earthquakes are plotted in Fig. 10.

Table 5A EB displacements and rotations of Bridge 1 for 1999 Kocaeli Earthquake

EB	Translation X (mm)	Translation Y (mm)	Translation Z (mm)	Rotation X (rad)	Rotation Y (rad)	Rotation Z (rad)
1	-12.776	0.000	-1.252	-0.00863	-0.01119	-0.00591
2	-9.451	0.000	0.511	-0.00817	-0.00915	-0.00674
3	-6.977	0.000	0.337	-0.00822	-0.00764	0.00721
4	5.235	0.000	0.264	-0.00836	-0.00652	0.00765
5	3.996	0.000	0.207	-0.00847	-0.00565	0.00787
6	-3.361	0.000	-0.169	-0.00849	0.00539	0.00783
7	-4.662	0.000	-0.243	-0.00844	0.00587	0.00757
8	-6.514	0.000	-0.337	-0.00835	0.00682	-0.00729
9	-9.097	0.000	-0.539	-0.00831	0.00852	-0.00694
10	12.890	0.000	-1.408	-0.00886	0.01100	-0.00628

Table 5B EB displacements and rotations of Bridge 1 for 1992 Erzincan Earthquake

EB	Translation X (mm)	Translation Y (mm)	Translation Z (mm)	Rotation X (rad)	Rotation Y (rad)	Rotation Z (rad)
1	-8.334	0.000	0.723	0.00436	-0.00841	-0.00235
2	-6.414	0.000	-0.346	0.00418	0.00704	-0.00248
3	5.664	0.000	-0.263	0.00420	0.00706	-0.00258
4	-5.612	0.000	-0.257	0.00421	0.00695	-0.00269
5	5.704	0.000	0.258	0.00419	-0.00726	-0.00293
6	5.971	0.000	0.290	0.00412	-0.00792	-0.00307
7	6.292	0.000	0.326	0.00411	-0.00863	-0.00312
8	-7.000	0.000	0.351	0.00414	-0.00928	-0.00310
9	-8.316	0.000	0.354	0.00419	0.01016	-0.00297
10	-10.204	0.000	0.756	0.00450	-0.01192	0.00277

Table 5C EB displacements and rotations of Bridge 1 for 1999 Duzce Earthquake

EB	Trans-lation X (mm)	Trans-lation Y (mm)	Trans-lation Z (mm)	Rotation X (rad)	Rotation Y (rad)	Rotation Z (rad)
1	-11.750	0.000	-1.1130	-0.0079	-0. 0101	-0. 0053
2	-8.580	0.000	0.468	-0. 00737	-0.00833	-0. 00615
3	-6.290	0.000	0. 306	-0. 00756	-0. 00695	0. 00660
4	4.812	0.000	0. 239	-0. 00757	-0. 00588	0. 00693
5	3.601	0.000	0. 186	-0. 00768	-0. 00511	0. 00709
6	-3.060	0.000	-0. 150	-0. 00778	0. 00492	0. 00718
7	-4.200	0.000	-0220	-0. 00764	0. 00535	0. 00686
8	-5.870	0.000	-0. 310	-0. 00765	0. 00617	-0. 00657
9	-8.350	0.000	-0490	-0. 00758	0. 00773	-0. 00635
10	11.668	0.000	-1.270	-0. 00811	0. 01011	-0. 00575

In the time history analyses, element matrices were computed using the Gauss numerical integration technique (Bathe 1996). The Newmark method was used in the solution of the equation of motion. The modified acceleration records were applied to all three directions of the bridges. Calculated element forces were used to evaluate the damage assessment, performance levels and seismic performance based on Turkish Seismic Code 2007.

3.3.1 Time history analysis results of bridge 1

Bridge 1 is a single span bridge and based on the Turkish Seismic Code, there is no need to evaluate the seismic performance of the frames in detail. Control of the structural stability of the elastomeric bearings (EB) is sufficient to assess the performance of the bridge. Tables 5A-C show the frame displacements of the elastomeric bearings which are under each of the precast I beams (See Figs. 2 and 3). As seen in Tables 5A-C, any displacement in the obtained time-history analyses does not exceed the allowed capacity of the elastomeric bearings.

3.3.2 Time history analysis results of bridge 2, bridge 3, and bridge 4

The element forces which occurred due to the 1999 Kocaeli Earthquake, 1992 Erzincan Earthquake and 1999 Duzce Earthquake on the bottom level of the piers for each bridge, are shown in Tables 6A-C, respectively.

Using the element forces shown in Tables 6A-C, input-capacity ratios were calculated based on Turkish Seismic Code 2007 and seismic performance levels were determined for Bridges 2-4. (See Tables 7A-C). When calculating the results, the example of Bridge 2, is given below. (For further explanation related to terms, see the "*Bases of Linear Seismic Performance According to Turkish Seismic Code 2007*" part of the study. Here, the area sections of the pier are given in Fig. 3 and bw, the width of section; *d*, useful height; fcm, concrete compression strength; and fctm, concrete tensile strength are considered as 1.8 m, 2.2 m, 25 MPa, and 3.9 MPa, respectively.

$$K_N = \frac{27.147}{9.96*25} = 0.11 \qquad K_V = \frac{15.780}{1.8*2.2*3.9} = 1.02$$

$$r(CapacityRatio) = \frac{M_e}{M_K - M_d} = \frac{112.495}{82.745} = 1.36$$

As shown in Tables 7A-C, during all three earthquakes, all the piers of the bridges (except Pier 1 of Bridge 3) are in the minimum damage region which stays under the regulatory minimums based on TSC 2007. Pier 1 of Bridge 3 goes between the minimum damage limit (ML) and the safety damage limit (SL) under the 1999 Kocaeli

Table 6A Element forces obtained on the bottom level of piers for 1999 Kocaeli earthquake

Bridge	Piers	Ne (kN)	V_e (kN)	M_k-M_d (kNm)	M_A (kNm)	M_E (kNm)
Bridge 2	Pier 1	27.147	15.780	82.745	82.745	112.495
Bridge 3	Pier 1	19.276	10.573	154.050	154.050	413.613
	Pier 2	23.022	8.961	162.500	162.500	366.598
	Pier 3	20.162	6.475	75.478	75.478	152.342
Bridge 4	Pier 1	24.089	-21.734	164.580	164.580	318.889
	Pier 2	24.095	-14.874	164.580	164.580	233.679

Table 6B Element forces obtained on the bottom level of piers for 1992 Erzincan earthquake

Bridge	Piers	Ne (kN)	V_e (kN)	M_k-M_d (kNm)	M_A (kNm)	M_E (kNm)
Bridge 2	Pier 1	25.224	14.264	82.745	82.745	106.390
Bridge 3	Pier 1	17.646	9.692	154.050	154.050	383.246
	Pier 2	21.233	8.084	162.500	162.500	339.529
	Pier 3	18.579	6.087	75.478	75.478	144.136
Bridge 4	Pier 1	22.867	-19.573	164.580	164.580	298.370
	Pier 2	22.631	-13.972	164.580	164.580	216.489

Table 6C Element forces obtained on the bottom level of piers for 1999 Duzce earthquake

Bridge	Piers	Ne (kN)	V_e (kN)	M_k-M_d (kNm)	M_A (kNm)	M_E (kNm)
Bridge 2	Pier 1	24.889	14.453	82.745	82.745	103.318
Bridge 3	Pier 1	17.496	9.677	154.050	154.050	372.571
	Pier 2	21.012	8.223	162.500	162.500	330.817
	Pier 3	18.485	5.947	75.478	75.478	137.466
Bridge 4	Pier 1	22.047	-19.83	164.580	164.580	292.347
	Pier 2	21.770	-13.541	164.580	164.580	214.429

Table 7A Seismic performance parameters of the piers for Kocaeli earthquake

Bridge	Piers	K_N	K_V	Capacity ratio (*r*)	Performance level
Bridge 2	Pier 1	0.11	1.02	1.36	ML
Bridge 3	Pier 1	0.08	0.69	2.68	ML-SL
	Pier 2	0.09	0.58	2.26	ML
	Pier 3	0.08	0.42	2.02	ML
Bridge 4	Pier 1	0.10	0.41	1.94	ML
	Pier 2	0.10	0.96	1.42	ML

Table 7B Seismic performance parameters of the piers for Erzincan earthquake

Bridge	Piers	K_N	K_V	Capacity ratio (*r*)	Performance level
Bridge 2	Pier 1	0.10	1.01	1.29	ML
Bridge 3	Pier 1	0.09	0.40	2.49	ML
	Pier 2	0.09	0.45	2.09	ML
	Pier 3	0.07	0.72	1.91	ML
Bridge 4	Pier 1	0.11	0.40	1.81	ML
	Pier 2	0.12	1.01	1.42	ML

Table 7C Seismic performance parameters of the piers for Düzce earthquake

Bridge	Piers	K_N	K_V	Capacity ratio (r)	Performance level
Bridge 2	Pier 1	0.10	1.01	1.25	ML
Bridge 3	Pier 1	0.09	0.63	2.42	ML
	Pier 2	0.09	0.53	2.04	ML
	Pier 3	0.07	0.40	1.82	ML
Bridge 4	Pier 1	0.11	0.40	1.78	ML
	Pier 2	0.10	1.01	1.25	ML

Earthquake, which is the distinctive damage region, which also stays under the regulatory minimums based on TSC 2007.

4. Conclusions

In this study, the seismic performance levels of four bridges are determined using finite element modeling based on ambient vibration testing. For the purpose, four prestressed precast I beam bridges constructed on the Ankara-Sivas railway line are selected for analytical and experimental studies. Firstly, 3D finite element models of the bridges are constituted using LARSA4D software and analytical dynamic characteristics are obtained. Then ambient vibration testing conducted on each bridge under natural excitations and experimental natural frequencies is estimated. Lastly, time history analyses of the bridges under three huge earthquakes which occurred on the North Anatolian Fault where the bridges are, are performed and seismic performance levels according to TSC (2007) are determined. The following observations and conclusions from the study can be made.

- The first three natural frequencies of the bridges provided from the finite element analyses are obtained between 1.62 and 8.56 Hz. The frequencies of the experimental analyses derived from ambient vibration testing are estimated between 2.42 and 8.58 Hz. Due to the accelerometers in the X direction not being taken, longitudinal modes are not obtained from AVT.
- Damping ratios changed between 0 and 3% for all bridges, which is acceptable for such structures.
- Mode shapes are obtained as longitudinal bending, vertical bending and torsional modes from both finite element analyses and ambient vibration testing.
- Due to little difference between analytical and experimental dynamic characteristics, the FEMs are assumed as accurate models for future analyses such as earthquakes.
- As Bridge 1 has only a single span, only the displacements that occurred on the elastomeric bearings obtained from the time history analysis are considered in assessing seismic performance levels and it is understood that the displacements are minimal compared to the allowed displacements. Thus, it is highlighted that Bridge 1 shows a good structural response against the 1999 Kocaeli Earthquake.
- The response of the piers of Bridge 2, Bridge 3 and Bridge 4 is investigated according to time history analysis results. K_N, K_V and r capacity ratio are calculated from the element forces occurring on the bottom of the piers to determine the seismic performance levels. It is clearly seen that the seismic performance levels are in the minimum damage region (ML).
- As a general result related to the seismic performance levels of the bridges, time history analyses show that damage assessment values are below the limits of the regulations for all bridges under the 1999 Kocaeli, 1992 Erzincan, and 1999 Düzce Earthquakes. The damage on the bridges is all under the minimum damage limit which is the minimum damage region (ML).

Acknowledgments

This research has been supported by Yıldız Technical University Scientific Research Projects Coordination Department. Project Number: 2011-05-01-YULAP (02.05. 2011-02.01.2015).

References

Altunışık, A.C., Bayraktar, A., Sevim, B. and Ateş, Ş. (2011a), “Ambient vibration based seismic evaluation of isolated Gülburnu highway bridge”, *Soil Dyn. Earthq. Eng.*, **31**(11), 1496-1510.

Altunışık, A.C., Bayraktar, A., Sevim, B. and Özdemir, H. (2011b), “Experimental and analytical system identification of eynel arch type steel highway bridge”, *J. Constr. Steel Res.*, **67**(12), 1912-1921.

ARTEMIS (2014), Structural Vibration Solutions A/S; Version 3, Aalborg East Denmark.

Asr, A.A., Javadi, A.A., Johari, A. and Chen, Y. (2014), “Lateral load bearing capacity modelling of piles in cohesive soils in undrained conditions: An intelligent evolutionary approach”, *Appl. Soft Comput.*, **24**, 822-828.

Bathe, K.J. (1996), *Finite Element Procedures in Engineering Analysis*, Prentice-Hall, NJ, USA.

Bayraktar, A., Altunışık, A.C., Sevim, B., Türker, T., Domaniç, A. and Taş, Y. (2009), “Vibration characteristics of Kömürhan highway bridge constructed with balanced cantilever method”, *J. Perform. Constr. Facil.*, **23**(2), 90-99.

Bendat, J. and Piersol, A. (1986), *Random Data: Analysis and Measurement Procedures*, (2nd Edition), John Wiley and Sons, USA.

Bendat, J.S. and Piersol, A.G. (2004), *Random Data: Analysis and Measurement Procedures*, John Wiley and Sons, USA.

Brincker, R., Zhang, L. and Andersen, P. (2000), “Modal identification from ambient responses using frequency domain decomposition”, *Proceedings of the 18th International Modal Analysis Conference*, San Antonio, TX, USA, February.

Brincker, R., Ventura, C.E. and Andersen, P. (2003), “Why output-only modal testing is a desirable tool for a wide range of practical applications”, *Proceedings of the 21st International Modal Analysis Conference* (*IMAC*), Kissimmee, FL, USA, February.

Butterworth, S. (1930), "On the theory of filter amplifiers", *Wireless Engineer*, **7**(6), 536-541.
Caetano, E. (2000), "Dynamic of cable-stayed bridges: Experimental assessment of cable-structure Interaction", Ph.D. Dissertation; Engineering Faculty of University of Porto, Portugal.
Camara, A. and Astiz, M.A. (2012), "Pushover analysis for the seismic response prediction of cable-stayed bridges under multi-directional excitation", *Eng. Struct.*, **41**, 444-455.
Casas, J.R. and Chambi, J.L. (2014), "Partial safety factors for CFRP-wrapped bridge piers: Model assessment and calibration", *Compos. Struct.*, **118**, 267-283.
Catalan, A., Climent, A.B. and Cahis, X. (2010), "Selection and scaling of earthquake records in assessment of structures in low-to-moderate seismicity zones", *Soil Dyn. Earthq. Eng.*, **30**(1-2), 40-49.
Chopra, A.K. (2006), *Dynamics of Structures: Theory and Applications to Earthquake Engineering*, (Third Edition), Prentice Hall, USA.
Dawood, H.M. and ElGawady, M. (2013), "Performance-based seismic design of unbonded precast post-tensioned concrete filled GFRP tube piers", *Compos. Part B: Eng.*, **44**(1), 357-367.
URL (2015), http://www.deprem.gov.tr/en/home; AFAD, Republic Of Turkey Prime Ministry Disaster & Emergency Management Authority Earthquake Department, Ankara, Turkey.
Dwairi, H.M., Wagner, M.C., Kowalsky, M.J. and Zia, P. (2010), "Behavior of instrumented prestressed high performance concrete bridge girders", *Constr. Build. Mater.*, **24**(11), 2294-2311.
El-Gawady, M.A. and Dawood, H.M. (2012), "Analysis of segmental piers consisted of concrete filled FRP tubes", *Eng. Struct.*, **38**, 142-152.
Gentile, C. and Bernardini, G. (2008), "Output-only modal identification of a reinforced concrete bridge from radar-based measurements", *NDT&E International*, **71**(7), 544-553.
Ghosh, G. and Singh, Y. (2011), "Thakkar SK. Seismic response of a continuous bridge with bearing protection devices", *Eng. Struct.*, **33**(4), 1149-1156.
Heo, G., Kim, C. and Lee, C. (2014), "Experimental test of asymmetrical cable-stayed bridges using MR-damper for vibration control", *Soil Dyn. Earthq. Eng.*, **57**, 78-85.
Herlufsen, H., Gade, S. and Møller, N. (2006), "Identification techniques for Operational Modal Analysis - An overview and practical experiences", *IMAC-XXIV: Conference & Exposition on Structural Dynamics*, St. Louis, MI, USA, January-February.
Jacobsen, N.J., Andersen, P. and Brincker, R. (2006), "Using enhanced frequency domain decomposition as a robust technique to harmonic excitation in operational modal analysis", *Proceedings of ISMA2006: International Conference on Noise &Vibration Engineering*, Leuven, Belgium, September.
Karmakar, D., Chaudhuri, S.R. and Shinozuka, M. (2012), "Seismic response evaluation of retrofitted Vincent Thomas Bridge under spatially variable ground motions", *Soil Dyn. Earthq. Eng.*, **42**, 119-127.
Kayhan, A.H., Korkmaz, K.A. and Irfanoglu, A. (2011), "Selecting and scaling real ground motion records using harmony search algorithm", *Soil Dyn. Earthq. Eng.*, **31**(7), 941-953.
Kim, D.H., Moon, D.Y., Kim, M.K., Zi, G. and Roh, H. (2015), "Experimental test and seismic performance of partial precast concrete segmental bridge column with cast-in-place base", *Eng. Struct.*, **100**, 178-188.
Kong, B., Cai, C.S. and Kong, X. (2015), "Field monitoring study of an integral abutment bridge supported by prestressed precast concrete piles on soft soils", *Eng. Struct.*, **104**, 18-31.
Kulpraphа, N. and Warnitchai, P. (2012), "Structural health monitoring of continuous prestressed concrete bridges using ambient thermal responses", *Eng. Struct.*, **40**, 20-38.
LARSA 4D, V7.07.16 (2013), Academic Version, Larsa, Inc., New York, NY, USA.
Lee, D.H., Park, J., Lee, K. and Kim, B.H. (2011), "Nonlinear seismic assessment for the post-repair response of RC bridge piers", *Compos. Part B: Eng.*, **42**(5), 1318-1329.
Mara, V., Haghani, R. and Harryson, P. (2014), "Bridge decks of fibre reinforced polymer (FRP): A sustainable solution", *Constr. Build. Mater.*, **50**, 190-199.
Marti, J.V., Vidosa, F.G., Yepes, V. and Alcala, J. (2013), "Design of prestressed concrete precast road bridges with hybrid simulated annealing", *Eng. Struct.*, **48**, 342-352.
Mayoral, J.M. and Romo, M.P. (2015), "Seismic response of bridges with massive foundations", *Soil Dyn. Earthq. Eng.*, **71**, 88-99.
Moravcik, M. (2013), "Modified system of prestressing for new precast girders developed for highway bridges", *Procedia Eng.*, **65**, 236-241.
Park, J. and Towashiraporn, P. (2014), "Rapid seismic damage assessment of railway bridges using the response-surface statistical model", *Struct. Safety*, **47**, 1-12.
Ramos, J.L.F.S. (2007), "Damage identification on masonry structures based on vibration signatures", Ph.D. Dissertation; University of Minho, Portugal.
Roh, H. and Reinhorn, A.M. (2010), "Hysteretic behavior of precast segmental bridge piers with superelastic shape memory alloy bars", *Eng. Struct.*, **32**(10), 3394-3403.
Roh, H., Ou, Y.C., Kim, J. and Kim, W. (2014), "Effect of yielding level and post-yielding stiffness ratio of ED bars on seismic performance of PT rocking bridge piers", *Eng. Struct.*, **81**, 454-463.
Ryu, H.K. and Chang, S.P. (2005), "Ultimate strength of continuous composite box-girder bridges with precast decks", *J. Constr. Steel Res.*, **61**(3), 329-343.
Sarrazin, M., Moroni, O., Neira, C. and Venegas, B. (2013), "Performance of bridges with seismic isolation bearings during the Maule earthquake, Chile", *Soil Dyn. Earthq. Eng.*, **47**, 117-131.
Schallhorn, C. and Rahmatalla, S. (2015), "Crack detection and health monitoring of highway steel-girder bridges", *Struct. Health Monitor.*, **14**(3), 281-299.
Sousa, H., Bento, J. and Figueiras, J. (2013), "Construction assessment and long-term prediction of prestressed concrete bridges based on monitoring data", *Eng. Struct.*, **52**, 26-37.
TSC (2007), Turkish Earthquake Resistant Design Code Specifications for buildings to be built in disaster areas; Ministry of Public Works & Settlement, Ankara, Turkey,
Valipour, H., Rajabi, A., Foster, S.J. and Bradford, M.A. (2015), "Arching behavior of precast concrete slabs in a deconstructable composite bridge deck", *Constr. Build. Mater.*, **87**, 67-77.
Wilson, T., Chen, S. and Mahmoud, H. (2015), "Analytical case study on the seismic performance of a curved and skewed reinforced concrete bridge under vertical ground motion", *Eng. Struct.*, **100**, 128-136.
Xiao, Y., Guo, Y.R., Zhu, P.S., Kunnath, S. and Martin, G.R. (2012), "Networked pseudo dynamic testing of bridge pier and precast pile foundation", *Eng. Struct.*, **38**, 32-41.
Yan, B., Dai, G.L. and Hu, N. (2015), "Recent development of design and construction of short span high-speed railway bridges in China", *Eng. Struct.*, **100**, 707-717.
Zacharenaki, A., Fragiadakis, M., Assimaki, D. and Papadrakakis, M. (2014), "Bias assessment in incremental dynamic analysis due to record scaling", *Soil Dyn. Earthq. Eng.*, **67**, 158-168.

CC